

DISPLACEMENTS REPRESENTATIONS FOR THE PROBLEMS WITH SPHERICAL AND CIRCULAR MATERIAL SURFACES WITH SURFACE TENSION

by SOFIA G. MOGILEVSKAYA and VOLODYMYR I. KUSHCH and ANNA Y. ZEMLYANOVA

*(Department of Civil, Environmental,
and Geo- Engineering, University of Minnesota,
500 Pillsbury Drive S.E.,
Minneapolis, MN, 55455, USA)*

*(Institute for Superhard Materials
of the National Academy of Sciences of Ukraine,
04074 Kiev, Ukraine)*

*(Department of Mathematics,
Kansas State University,
138 Cardwell Hall,
Manhattan, Kansas, 66506, USA)*

[Received XX.XX.XX. Revise XX.XX.XX]

Summary

The displacements representations of the type used by Christensen and Lo (1979) are modified to allow for analytical treatment of problems involving spherical and circular material surfaces that possess constant surface tension. The modified representations are used to derive closed-form expressions for the local elastic fields and effective moduli of a macroscopically isotropic composite materials containing spherical and circular inhomogeneities with the interfaces described by the complete Gurtin-Murdoch and Steigmann-Ogden models.

Keywords: Circular and spherical inhomogeneities, Christensen-Lo solutions, Gurtin-Murdoch and Steigmann-Ogden models, Effective properties

1. Introduction

In their paper, Christensen and Lo (1979) presented new micromechanical scheme, the generalized self-consistent scheme, for the evaluation of the effective shear moduli of macroscopically isotropic composites containing cylindrical and spherical inhomogeneities. The scheme utilizes the three phases model that involves a spherical or circular inhomogeneity, a spherical or circular annulus of matrix material, and an infinite outer region of equivalent homogeneous material subjected to uniform far-field load.

For the case of arbitrary load, the rigorous solution of such model problem would involve the use of infinite series (inner and outer spherical harmonics in three dimensions or Laurent and Taylor series in two dimensions) and could be quite complex. Instead, Christensen and Lo (1979) suggested to use the closed-form representations for the displacements in spherical and cylindrical coordinate systems for the special far-field load - simple shear. The

representations were not new; they have been used earlier for various problems involving spherical or circular boundaries, see Love (1927) for the three-dimensional case and Savin (1961) for the two-dimensional one. However, they became much more popular after publication of Christensen and Lo (1979) paper and have been extensively used for the problems involving inhomogeneities with interphases, imperfect interfaces, and material surfaces, see e.g. Benveniste et al. (1989), Herve and Zaoui (1993), Duan et al. (2006), Xu et al. (2016), Zemlyanova and Mogilevskaya (2018a), among many others.

We note that another type of displacement representations for the axisymmetric problems with spherical surfaces was suggested in e.g. Goodier (1933), see also Lurie (1964), and used for the problems with imperfect interfaces and material surfaces in e.g. Duan et al. (2005, 2007), He and Li (2006), Lim et al. (2006), Mi and Kouris (2006). While the solution for the case of simple shear far-field load can be obtained from the superposition of the appropriately chosen axisymmetric solutions, see e.g. Hashin (1991), the related procedure requires an additional step and the derivations associated with that step.

One limitation of Christensen and Lo (1979) type representations is that they are not valid for the problems with surface and interface effects as they do not include surface tension. Another limitation is that they involve unknown coefficients, which in many cases have to be found numerically from the system of linear algebraic equations, thus not allowing for accurate identification of all governing problem parameters.

The concept of surface tension is important in modeling of various nano-sized phenomena where the influence of the surface becomes more significant due to the high surface-area-to-volume ratio, see e.g. Cahn and Larch (1982), Miller and Shenoy (2000), Sharma and Ganti (2002, 2004), Sharma et al. (2003), Dingreville et al. (2005), Lim et al. (2006), He and Li (2006), Huang and Wang (2006), Mi and Kouris (2006), Mogilevskaya et al. (2008, 2010), Ru (2010), Chhapadia et al (2011), Kushch et al. (2011, 2013), Chatzigeorgiou et al. (2017), Javili et al. (2017), and many others.

The models proposed by Gurtin-Murdoch (1975, 1978) and Steigmann-Ogden (1997, 1999) are the most studied continuum models of material surfaces with surface tension. In these models, the interface between the material constituents is treated as either a membrane (Gurtin-Murdoch model) or a shell (Steigmann-Ogden model) of vanishing thickness possessing surface tension as well as corresponding surface elastic properties.

Only a few closed-form solutions of the inhomogeneity problems involving the *complete* Gurtin-Murdoch model have been reported so far, perhaps due notorious difficulties in handling effects introduced by surface tension. Quite naturally, the benchmark problems, for which analytical solutions could be constructed, involve regular shapes of material surfaces. These solutions have been reported for the case of circular inhomogeneity in e.g. Mogilevskaya et al. (2008), Jammes et al. (2009), for elliptical inhomogeneity in Kushch et al. (2014), for spherical inhomogeneity in Lim et al. (2006), He and Li (2006), Kushch et al. (2011, 2013), and spheroidal inhomogeneity in Kushch (2018), Kushch et al. (2018). The methods used in these publications were quite complex, which was justified for the problems involving multiple inhomogeneities. However, for the important case of a single inhomogeneity, often used in various single-inhomogeneity-based homogenization schemes, it is desirable to devise simpler solution by modifying the representations used by Christensen and Lo (1979).

To the best knowledge of the authors, no publication reports the solution of the problem of a spherical inhomogeneity with the interface described by the *complete* Steigmann-Ogden

model (with a full set of interface parameters) and non-hydrostatic loading conditions. The first and the only publication that considered the Steigmann-Ogden model for spherical inhomogeneity was by Zemlyanova and Mogilevskaya (2018a) who presented the solutions for two *particular* cases: (i) hydrostatic load (when the problem becomes one-dimensional) and (ii) deviatoric load & zero surface tension (when the problem can be solved by using classical Christensen and Lo type displacement representations). As stated above, the latter representations are not valid for the cases involving surface tension and that was the reason why the authors of that work have not been able to solve the problem in more general setting. The two-dimensional solutions for the problem of circular inhomogeneities with the complete Steigmann-Ogden interface model are reported in Zemlyanova and Mogilevskaya (2018b) and Han et al. (2018). However, they too were obtained with tedious algebra that, for the case of a single inhomogeneity, could be avoided, if simpler representations of the type used by Christensen and Lo (1979) could be modified to include surface tension.

Thus, the goal of the present paper is three-fold. First, we present *new* Christensen and Lo (1979) type *representations* to allow for simple analytical solutions of the problems involving spherical and circular material surfaces possessing constant surface tension. Second, using the obtained representations, we derive *new analytical solution* for the problem of a spherical inhomogeneity with the interface described by the *complete* Steigmann-Ogden model. Finally, we provide *closed-form analytical expressions* for the coefficients involved in those representations for the cases of the complete Gurtin-Murdoch and Steigmann-Ogden models. We emphasize again that the focus of the present paper is not on the modification of micromechanical scheme of Christensen and Lo (1979) but rather on the representations they used to obtain it. The new representations devised here could be used in variety of micromechanical schemes one of which, Maxwell's (1873) homogenization scheme, is used in the present paper.

The paper is structured as follows. In Section 2, we review the Christensen and Lo representations for the case of simple shear far-field load and, for completeness, provide similar representation for the case of hydrostatic load. In Section 3 (with the details provided in Appendix A), we use analytical solutions for the problems of a circular inhomogeneity with the complete Gurtin-Murdoch (Mogilevskaya et al., 2008) and Steigmann-Ogden (Zemlyanova and Mogilevskaya, 2018b) interfaces to construct the Christensen and Lo (1979) type representations for the hydrostatic and simple shear far-field loads. In Section 4 (with the details provided in Appendix B), we use analytical solution of Kushch et al. (2011) to presents analogous representations for the problem of a spherical inhomogeneity with the complete Gurtin-Murdoch interface. In Section 5, we use the representations of Section 4 to obtain new analytical solution for the problem of a spherical inhomogeneity with the interface described by the complete Steigmann-Ogden model. In Section 6, we use this solution in combination with Maxwell's (1873) methodology to derive the single-inhomogeneity based estimate of the effective shear modulus of macroscopically isotropic material containing spherical inhomogeneities with interfaces described by the complete Steigmann-Ogden model. In Section 7, we present a summary of our results and conclusions.

2. Christensen and Lo (1979) representations for circular and spherical inhomogeneities

Consider the problem of a circular (Fig.1a) or a spherical (Fig.1b) inhomogeneity of radius R embedded into an infinite matrix and subjected to uniform far field load σ_{kj}^∞ , $k, j = 1, \dots, d$, where $d = 2$ in two dimensions and $d = 3$ in three dimensions. The center of the inhomogeneity is located at the origin of the Cartesian coordinate system. Assume also that the bulk material of the matrix (inhomogeneity) is linearly elastic and isotropic; the corresponding elastic moduli for the two phases are shear modulus $\mu(\mu_I)$ and Poisson's ratio $\nu(\nu_I)$. The interface conditions between the matrix and inhomogeneity are not specified at this time.

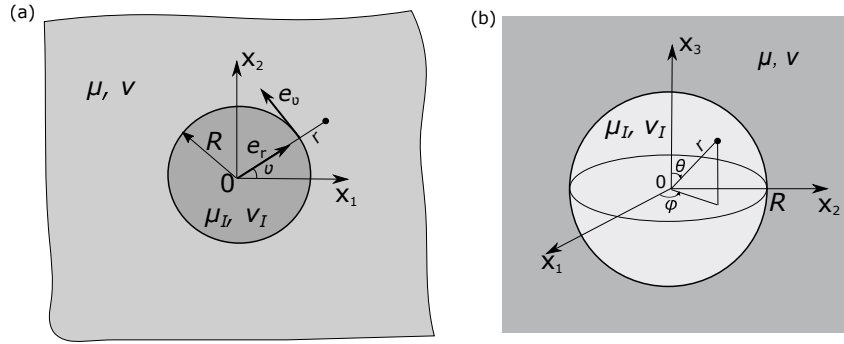


Fig. 1 a) Circular and b) spherical inhomogeneity in an infinite matrix

Christensen and Lo (1979) used the following representations for the displacements in the polar or spherical coordinate systems of Fig.1 and the case of simple shear far-field load (the only non-vanishing far-field stresses are $\sigma_{11}^\infty = -\sigma_{22}^\infty = \sigma_d^\infty$):

- circular inhomogeneity

inside the inhomogeneity

$$u_r(z) = \frac{R}{4\mu_I} \left[d_1 \frac{r}{R} + (\kappa_I - 3) a_1 \frac{r^3}{R^3} \right] \cos 2\vartheta \quad (2.1)$$

$$u_\vartheta(z) = \frac{R}{4\mu_I} \left[-d_1 \frac{r}{R} + (\kappa_I + 3) a_1 \frac{r^3}{R^3} \right] \sin 2\vartheta$$

inside the matrix

$$u_r(z) = \frac{R}{4\mu} \left[2\sigma_d^\infty \frac{r}{R} + (\kappa + 1) a_3 \frac{R}{r} + c_3 \frac{R^3}{r^3} \right] \cos 2\vartheta \quad (2.2)$$

$$u_\vartheta(z) = \frac{R}{4\mu} \left[-2\sigma_d^\infty \frac{r}{R} - (\kappa - 1) a_3 \frac{R}{r} + c_3 \frac{R^3}{r^3} \right] \sin 2\vartheta$$

in which $\kappa = 3 - 4\nu$, $\kappa_I = 3 - 4\nu_I$, and the unknown coefficients d_1 , a_1 , a_3 , c_3 are found from the interface and far-field conditions. It should be noted that the expressions of Eq. (4.1) in Christensen and Lo (1979) were dimensionally inconsistent, so in Eq. (2.2) we added missing multipliers to eliminate this inconsistency.

- spherical inhomogeneity

$$\begin{aligned} u_r &= U_r(r) \sin^2 \theta \cos 2\varphi \\ u_\theta &= U_\theta(r) \sin \theta \cos \theta \cos 2\varphi \\ u_\varphi &= -U_\theta(r) \sin \theta \sin 2\varphi \end{aligned} \quad (2.3)$$

in which the functions $U_r(r)$, $U_\theta(r)$ of Eq. (2.3) are different for the inhomogeneity and the matrix and taken as

inside the inhomogeneity

$$\begin{aligned} U_r^{inh}(r) &= A_1 r - \frac{6\nu_I}{1 - 2\nu_I} A_2 r^3 \\ U_\theta^{inh}(r) &= A_1 r - \frac{7 - 4\nu_I}{1 - 2\nu_I} A_2 r^3 \end{aligned} \quad (2.4)$$

inside the matrix

$$\begin{aligned} U_r^{mat}(r) &= D_1 r + \frac{3D_3}{r^4} + \frac{5 - 4\nu}{1 - 2\nu} \frac{D_4}{r^2} \\ U_\theta^{mat}(r) &= D_1 r - \frac{2D_3}{r^4} + 2 \frac{D_4}{r^2} \end{aligned} \quad (2.5)$$

and involve five unknown coefficients A_1 , A_2 , D_1 , D_3 , D_4 that have to be found from the interface and far-field conditions.

Note that the representations of Eqs. (2.1)-(2.5) are not valid for the problems with surface tension. We add also that Christensen and Lo (1979) considered a three-phase model and their set of representations included expressions for the displacements inside the third phase (interphase), which is not present in the problems under study that deal with material surfaces of vanishing thicknesses.

For the completeness, we also list here the representations for the case of hydrostatic load (the only non-vanishing far-field stresses are $\sigma_{kk}^\infty = \sigma_h^\infty$, $k = 1, \dots, d$). Such representations are often used for the evaluation of the effective bulk modulus. The problem is one-dimensional and the expressions for the only non-vanishing radial component of the displacements are

- inside the inhomogeneity

$$u_r(z) = F_1 r \quad (2.6)$$

- inside the matrix

$$u_r(z) = F_2 r + F_3 / r^{d-1} \quad (2.7)$$

where again d is the dimension of the problem and the three unknown coefficients F_1 , F_2 , F_3 have to be found from the interface and far-field conditions.

3. Representations for a circular inhomogeneity with the Gurtin-Murdoch and Steigmann-Ogden interfaces

Consider circular inhomogeneity shown on Fig.1a. In both models, the displacements are continuous across the interface but the tractions undergo jumps. The tractions jump conditions for the more general Steigmann-Ogden model (characterized by the elastic parameters μ_0 , λ_0 , surface tension σ_0 , and bending parameters ζ_0 and χ_0) can be written as, see Zemlyanova and Mogilevskaya (2018b)

$$\begin{aligned} \sigma_{rr}^{inh} - \sigma_{rr}^{mat} &= -\frac{\sigma_0}{R} + \frac{\sigma_0}{R^2} (u_{r,\vartheta\vartheta} - u_{\vartheta,\vartheta}) \\ &\quad - (\lambda_0 + 2\mu_0) \frac{1}{R^2} (u_{\vartheta,\vartheta} + u_r) \\ &\quad - (2\chi_0 + \zeta_0) \frac{1}{R^4} (u_{r,\vartheta\vartheta\vartheta} - u_{\vartheta,\vartheta\vartheta}) \end{aligned} \quad (3.1)$$

$$\begin{aligned} \sigma_{r\vartheta}^{inh} - \sigma_{r\vartheta}^{mat} &= \frac{\sigma_0}{R^2} (u_{r,\vartheta} - u_{\vartheta}) \\ &\quad + (\lambda_0 + 2\mu_0) \frac{1}{R^2} (u_{\vartheta,\vartheta\vartheta} + u_{r,\vartheta}) \\ &\quad - (2\chi_0 + \zeta_0) \frac{1}{R^4} (u_{r,\vartheta\vartheta\vartheta} - u_{\vartheta,\vartheta\vartheta}) \end{aligned} \quad (3.2)$$

in which u_r and u_{ϑ} are local components of the surface displacements in the local coordinate system (r, ϑ) shown in Fig 1a, σ_{rr} , $\sigma_{r\vartheta}$ are the corresponding components of tractions in that system, and the subscript “,” indicates differentiation, e.g. $u_{\vartheta,\vartheta} = \partial u_{\vartheta} / \partial \vartheta$.

The tractions jump conditions for the Gurtin-Murdoch model could be recovered from Eqs. (3.1), (3.2) by assuming that the bending parameters vanish, i.e. $\zeta_0 = 0$ and $\chi_0 = 0$.

If the entire system is subjected to uniform far-field load, both problems can be solved analytically using complex variables formalism, see Mogilevskaya et al. (2008), Zemlyanova and Mogilevskaya (2018b). Using these solutions (briefly reviewed in Appendix A) and some algebra, the polar coordinates of the displacements everywhere in the composite system can be expressed in the following closed forms:

inside the inhomogeneity

$$\begin{aligned} u_r &= -\frac{\sigma_0}{2(K_I^{(2)} + \mu + 2\eta)} \frac{r}{R} + \frac{R}{4\mu_I} \left[d_1 \frac{r}{R} + (\kappa_I - 3) a_1 \frac{r^3}{R^3} \right] \cos 2\vartheta \\ u_{\vartheta} &= \frac{R}{4\mu_I} \left[-d_1 \frac{r}{R} + (\kappa_I + 3) a_1 \frac{r^3}{R^3} \right] \sin 2\vartheta \end{aligned} \quad (3.3)$$

inside the matrix

$$\begin{aligned}
u_r &= -\frac{\sigma_0}{2\left(K_I^{(2)} + \mu + 2\eta\right)} \frac{R}{r} + \frac{R}{4\mu} \left[2\sigma_d^\infty \frac{r}{R} + (\kappa + 1) a_3 \frac{R}{r} + c_3 \frac{R^3}{r^3} \right] \cos 2\vartheta \\
u_\vartheta &= \frac{R}{4\mu} \left[-2\sigma_d^\infty \frac{r}{R} - (\kappa - 1) a_3 \frac{R}{r} + c_3 \frac{R^3}{r^3} \right] \sin 2\vartheta
\end{aligned} \tag{3.4}$$

in which $K_I^{(2)} = 2\mu_I / (\kappa_I - 1)$ is the two-dimensional bulk modulus of the inhomogeneity,

$$\begin{aligned}
d_1 &= \frac{4\mu_I}{\kappa_I} \left(3 \frac{A_3}{R} + \kappa_I \frac{A_{-1}}{R} \right) \\
a_1 &= \frac{4\mu_I}{\kappa_I} \frac{A_3}{R} \\
a_3 &= \frac{4}{\kappa + 1} \left(3\eta^{(2)} \frac{A_3}{R} - \omega^{(1)} \frac{A_{-1}}{R} \right) \\
c_3 &= \frac{4}{\kappa + 1} \left[\left(\omega^{(1)} + \kappa\eta^{(2)} \right) \frac{A_{-1}}{R} - \omega^{(2)} \frac{A_3}{R} \right]
\end{aligned} \tag{3.5}$$

and the coefficients A_{-1} , A_3 are given, for the case of simple shear far-field load, by the last two expressions of Eqs. (A16) of Appendix A. The meanings of remaining parameters involved in Eqs. (3.3)-(3.5) are also explained in that appendix.

It follows from the representations of Eqs. (3.3), (3.4) that the only difference between them and those of Christensen and Lo (1979) are in radial components of the displacements, which now has the following forms:

$$u_r = u_r^{C-L} + A\sigma_0 \left(\frac{r}{R} \right)^p \tag{3.6}$$

where $A = -\frac{1}{2(K_I^{(2)} + \mu + 2\eta)}$, $p = 1$ inside the inhomogeneity, $p = -1$ inside the matrix and u_r^{C-L} are given by Eqs. (2.1), (2.2).

From Eq. (A4) of Appendix A, it follows that, for the case of hydrostatic far-field load $\sigma_{11}^\infty = \sigma_{22}^\infty = \sigma_h^\infty$, $\sigma_{12}^\infty = 0$, the coefficients involved in Eqs. (A7), (A8) of that appendix are

$$ReA_1 = \frac{R}{2\left(K_I^{(2)} + \mu + 2\eta\right)} \left(\frac{\kappa + 1}{2} \sigma_h^\infty - \frac{\sigma_0}{R} \right), \quad A_{-1} = A_3 = 0 \tag{3.7}$$

Substitution of the coefficients of Eqs. (3.7) into Eqs. (A7), (A8) leads to the representations for the displacements given by Eqs. (2.6), (2.7) with $d = 2$ and the following coefficients F_1 , F_2 , F_3 :

$$\begin{aligned}
F_1 &= \frac{1}{2(K_I^{(2)} + \mu + 2\eta)} \left(\frac{\kappa + 1}{2} \sigma_h^\infty - \frac{\sigma_0}{R} \right) \\
F_2 &= \frac{\sigma_h^\infty}{2K^{(2)}} \\
F_3 &= -\frac{R^2}{2(K_I^{(2)} + \mu + 2\eta)} \left[\sigma_h^\infty \left(\frac{K_I^{(2)}}{K^{(2)}} - 1 + \frac{2\eta}{K^{(2)}} \right) + \frac{\sigma_0}{R} \right]
\end{aligned} \tag{3.8}$$

where $K^{(2)} = 2\mu/(\kappa - 1)$ is two-dimensional bulk modulus of the matrix.

4. Representations for a spherical inhomogeneity with the Gurtin-Murdoch material surface

Consider spherical inhomogeneity shown on Fig.1b. In the Gurtin-Murdoch model, the displacements are continuous across the interface but the tractions undergo jumps. The tractions jump conditions for the model (in which the interface is characterized by the elastic parameters μ_0 , λ_0 and the surface tension σ_0) can be written as, see Kushch et al. (2013), Zemlyanova and Mogilevskaya (2018a), (the latter paper had a misprint, missing term $T_{\theta r}$ in Eq. (4.2))

$$\sigma_{rr}^{inh} - \sigma_{rr}^{mat} = \frac{1}{r \sin \theta} [T_{\varphi r, \varphi} + T_{\theta r} \cos \theta + (T_{\theta r, \theta} - T_{\varphi \varphi} - T_{\theta \theta}) \sin \theta] \tag{4.1}$$

$$\sigma_{r\theta}^{inh} - \sigma_{r\theta}^{mat} = \frac{1}{r \sin \theta} [T_{\varphi \theta, \varphi} + (T_{\theta \theta, \theta} + T_{\theta r}) \sin \theta + (T_{\theta \theta} - T_{\varphi \varphi}) \cos \theta] \tag{4.2}$$

$$\sigma_{r\varphi}^{inh} - \sigma_{r\varphi}^{mat} = \frac{1}{r \sin \theta} [T_{\varphi \varphi, \varphi} + (T_{\theta \varphi, \theta} + T_{\varphi r}) \sin \theta + (T_{\varphi \theta} + T_{\theta \varphi}) \cos \theta] \tag{4.3}$$

in which

$$T_{\theta \theta} = \sigma_0 + \frac{\lambda_0 + \sigma_0}{r \sin \theta} (u_{\varphi, \varphi} + u_\theta \cos \theta + u_r \sin \theta) + \frac{\lambda_0 + 2\mu_0}{r} (u_{\theta, \theta} + u_r) \tag{4.4}$$

$$T_{\varphi \varphi} = \sigma_0 + \frac{\lambda_0 + 2\mu_0}{r \sin \theta} (u_{\varphi, \varphi} + u_\theta \cos \theta + u_r \sin \theta) + \frac{\lambda_0 + \sigma_0}{r} (u_{\theta, \theta} + u_r) \tag{4.5}$$

$$T_{\varphi \theta} = \frac{1}{r \sin \theta} [\mu_0 (u_{\theta, \varphi} - u_\varphi \cos \theta) + (\mu_0 - \sigma_0) u_{\varphi, \theta} \sin \theta] \tag{4.6}$$

$$T_{\theta \varphi} = \frac{1}{r \sin \theta} [(\mu_0 - \sigma_0) (u_{\theta, \varphi} - u_\varphi \cos \theta) + \mu_0 u_{\varphi, \theta} \sin \theta] \tag{4.7}$$

$$T_{\theta r} = \frac{\sigma_0}{r} (u_{r, \theta} - u_\theta) \tag{4.8}$$

$$T_{\varphi r} = \frac{\sigma_0}{r \sin \theta} (u_{r, \varphi} - u_\varphi \sin \theta) \tag{4.9}$$

If the entire system is subjected to uniform far-field load, the problem can be solved analytically using the technique of vector spherical harmonics, see Kushch (2013), Kushch et al. (2011). In that technique, the displacement vector in spherical coordinates is sought

as a linear combination of vector partial solutions of the Lam equation of isotropic elasticity and the coefficients involved in the combination are found from the boundary conditions.

For the case of simple shear far-field load, the only non-zero components are $\sigma_{11}^\infty = -\sigma_{22}^\infty = \sigma_d^\infty$, the displacement vector fields $\mathbf{u}(u_r, u_\theta, u_\varphi)$ can be represented inside the inhomogeneity and matrix as

inside the inhomogeneity ($|\mathbf{x}| = r < R$)

$$\mathbf{u}(\mathbf{x}) = \frac{3}{2(1-2\nu_I)} A_0 \mathbf{u}_{00}^{(3)}(\mathbf{x}) + 4A_1 \text{Re} \mathbf{u}_{22}^{(1)}(\mathbf{x}) - \frac{84}{1-2\nu_I} A_2 \text{Re} \mathbf{u}_{22}^{(3)}(\mathbf{x}), \quad (4.10)$$

inside the matrix ($|\mathbf{x}| = r > R$)

$$\mathbf{u}(\mathbf{x}) = 2 \frac{\sigma_d^\infty}{\mu} \text{Re} \mathbf{u}_{22}^{(1)}(\mathbf{x}) + D_0 \mathbf{U}_{00}^{(1)}(\mathbf{x}) - \frac{D_3}{3} \text{Re} \mathbf{U}_{22}^{(1)}(\mathbf{x}) + \frac{D_4}{1-2\nu} \text{Re} \mathbf{U}_{22}^{(3)}(\mathbf{x}), \quad (4.11)$$

with A_0, A_1, A_2 and D_0, D_3, D_4 being the unknown constants and $\mathbf{u}_{kk}^{(m)}(\mathbf{x}), \mathbf{U}_{kk}^{(m)}(\mathbf{x})$ being the vector partial solutions of the Lamé equation in spherical coordinates. These functions are given by Eqs. (B1), (B2) of Appendix B.

After some algebra that involves the use of Eqs. (B1)-(B3) of Appendix B, one arrives at the following component representations of Eqs. (4.10), (4.11):

inside the inhomogeneity

$$u_r = -rA_0 + U_r^{inh}(r) \sin^2 \theta \cos 2\varphi, \quad (4.12)$$

$$u_\theta = U_\theta^{inh}(r) \sin \theta \cos \theta \cos 2\varphi, \quad (4.13)$$

$$u_\varphi = -U_\theta^{inh}(r) \sin \theta \sin 2\varphi, \quad (4.14)$$

inside the matrix

$$u_r = -\frac{1}{r^2} D_0 + U_r^{mat}(r) \sin^2 \theta \cos 2\varphi \quad (4.15)$$

$$u_\theta = U_\theta^{mat}(r) \sin \theta \cos \theta \cos 2\varphi, \quad (4.16)$$

$$u_\varphi = -U_\theta^{mat}(r) \sin \theta \sin 2\varphi, \quad (4.17)$$

in which $U_r^{inh}(r), U_r^{mat}(r)$ are the functions defined in Eqs. (2.4), (2.5) with $D_1 = \sigma_d^\infty / 2\mu$. The remaining coefficients involved in Eqs. (4.12)-(4.17) can be found from the system of Eqs. (B5)-(B7) presented in Appendix B.

It can be seen that the only difference between the representations of Eqs. (4.12)-(4.17) and those of Christensen and Lo (1979) is in radial displacements, which now have the following forms that involve additional terms due to surface tension:

$$u_r = u_r^{C-L} + A\sigma_0 \left(\frac{r}{R}\right)^p \quad (4.18)$$

where $A = -\frac{2}{4\mu + 3K_I^{(3)} + 2\eta_0}$, $K_I^{(3)} = \frac{2}{3}\mu_I(1 + \nu_I)/(1 - 2\nu_I)$ is three-dimensional bulk modulus of the inhomogeneity, $p = 1$ inside the inhomogeneity, $p = -2$ inside the matrix, u_r^{C-L} are given by Eqs. (2.3)- (2.5), and

$$\eta_0 = (2\mu_0 + 2\lambda_0 + \sigma_0) / R \quad (4.19)$$

For the case of hydrostatic far-field load ($\sigma_{kk}^\infty = \sigma_h^\infty$, $\sigma_{kj}^\infty = 0$, $k \neq j$), the representations for the displacements are given by Eqs. (2.6), (2.7) with $d = 3$ and the following coefficients:

$$\begin{aligned} F_1 &= \frac{[1 + 4\mu / (3K^{(3)})] \sigma_h^\infty - 2\sigma_0/R}{4\mu + 3K_I^{(3)} + 2\eta_0} \\ F_2 &= \frac{\sigma_h^\infty}{3K^{(3)}} \\ F_3 &= R^3 \frac{\sigma_h^\infty \left[\left(1 - K_I^{(3)}/K^{(3)}\right) - 2\eta_0 / (3K^{(3)}) \right] - 2\sigma_0/R}{4\mu + 3K_I^{(3)} + 2\eta_0} \end{aligned} \quad (4.20)$$

where $K^{(3)} = \frac{2}{3}\mu(1 + \nu) / (1 - 2\nu)$ is three-dimensional bulk modulus of the matrix.

5. New solutions for a spherical inhomogeneity with the Steigmann-Ogden material surface (simple shear far-field load)

Consider again spherical inhomogeneity shown on Fig.1b but now assume that its interface is described by the complete Steigmann-Ogden model that includes surface tension. In this case, the jump of tractions on the spherical boundary can be written as, see Zemlyanova and Mogilevskaya (2018a):

$$\sigma_{rr}^{inh} - \sigma_{rr}^{mat} = \frac{1}{r \sin \theta} [T_{\varphi r, \varphi} + T_{\theta r} \cos \theta + (T_{\theta r, \theta} - T_{\varphi \varphi} - T_{\theta \theta}) \sin \theta] + \quad (5.1)$$

$$\begin{aligned} &\frac{1}{r^2 \sin^2 \theta} [M_{\varphi \varphi, \varphi \varphi} + (M_{\theta \varphi, \theta \varphi} + M_{\varphi \theta, \varphi \theta}) \sin \theta + M_{\theta \theta, \theta \theta} \sin^2 \theta + (M_{\varphi \theta, \varphi} + M_{\theta \varphi, \varphi}) \cos \theta + \\ &\quad (2M_{\theta \theta, \theta} - M_{\varphi \varphi, \theta}) \cos \theta \sin \theta - (M_{\theta \theta} - M_{\varphi \varphi}) \sin^2 \theta] \end{aligned}$$

$$\sigma_{r\theta}^{inh} - \sigma_{r\theta}^{mat} = \frac{1}{r \sin \theta} [T_{\varphi \theta, \varphi} + (T_{\theta \theta, \theta} + T_{\theta r}) \sin \theta + (T_{\theta \theta} - T_{\varphi \varphi}) \cos \theta] + \quad (5.2)$$

$$\frac{1}{r^2 \sin \theta} [M_{\varphi \theta, \varphi} + (M_{\theta \theta} - M_{\varphi \varphi}) \cos \theta + M_{\theta \theta, \theta} \sin \theta]$$

$$\sigma_{r\varphi}^{inh} - \sigma_{r\varphi}^{mat} = \frac{1}{r \sin \theta} [T_{\varphi \varphi, \varphi} + (T_{\theta \varphi, \theta} + T_{\varphi r}) \sin \theta + (T_{\varphi \theta} + T_{\theta \varphi}) \cos \theta] + \quad (5.3)$$

$$\frac{1}{r^2 \sin \theta} [M_{\varphi \varphi, \varphi} + (M_{\varphi \theta} + M_{\theta \varphi}) \cos \theta + M_{\theta \varphi, \theta} \sin \theta]$$

in which the components of the surface stress tensor \mathbf{T} are given by Eqs. (4.4)-(4.9), and the components of the surface couple-stress tensor \mathbf{M} are

$$M_{\varphi \varphi} = (2\chi_0 + \zeta_0)\kappa_{\varphi \varphi} + \zeta_0\kappa_{\theta \theta} \quad (5.4)$$

$$M_{\varphi \theta} = M_{\theta \varphi} = 2\chi_0\kappa_{\varphi \theta} \quad (5.5)$$

$$M_{\theta \theta} = \zeta_0\kappa_{\varphi \varphi} + (2\chi_0 + \zeta_0)\kappa_{\theta \theta} \quad (5.6)$$

$$\kappa_{\varphi \varphi} = -\frac{1}{r^2 \sin^2 \theta} [u_{r, \varphi \varphi} - u_{\varphi, \varphi} \sin \theta + (u_{r, \theta} - u_\theta) \cos \theta \sin \theta] \quad (5.7)$$

$$\kappa_{\varphi\theta} = \kappa_{\theta\varphi} = \frac{1}{2r^2 \sin^2 \theta} \left[(u_{r,\varphi\theta} - u_{\theta,\varphi}) \sin \theta - (u_{r,\varphi} - u_{\varphi} \sin \theta) \cos \theta + \frac{\partial}{\partial \theta} \left(\frac{u_{r,\varphi}}{\sin \theta} - u_{\varphi} \right) \sin^2 \theta \right] \quad (5.8)$$

$$\kappa_{\theta\theta} = \frac{1}{r^2} (u_{r,\theta\theta} - u_{\theta,\theta}) \quad (5.9)$$

Eqs. (5.4)-(5.9) involve the components of the tensor of changes of curvature $\boldsymbol{\kappa}$ and the bending stiffness parameters χ_0, ζ_0 .

Now, assuming simple shear load at infinity, we propose to use the representations of Eqs. (4.12)-(4.17) for obtaining the new solution for the problem of a spherical inhomogeneity with the complete Steigmann-Ogden interface. In Zemlyanova and Mogilevskaya (2018a), the solution for the simple shear far-field load was only presented for the case of zero surface tension.

Substitution of the representations of Eqs. (4.12)-(4.17) into Eqs. (5.1)-(5.3) leads to the following expressions for the jumps of boundary tractions:

$$\begin{aligned} \sigma_{r\varphi}^{inh} - \sigma_{r\varphi}^{mat} &= \left[\frac{2}{r^2} ((3\lambda_0 + 5\mu_0 + \sigma_0)U_\theta - 2(\mu_0 + \lambda_0 + \sigma_0)U_r) - 2\gamma \frac{R^3}{r^4} (2U_r - U_\theta) \right] \sin \theta \sin 2\varphi \\ \sigma_{r\theta}^{inh} - \sigma_{r\theta}^{mat} &= \\ \left[\frac{1}{r^2} (-(3\lambda_0 + 5\mu_0 + \sigma_0)U_\theta + 2(\mu_0 + \lambda_0 + \sigma_0)U_r) + \gamma \frac{R^3}{r^4} (2U_r - U_\theta) \right] \sin 2\theta \cos 2\varphi & \quad (5.10) \\ \sigma_{rr}^{inh} - \sigma_{rr}^{mat} &= -\frac{2\sigma_0}{r} + \\ \left[\frac{1}{r^2} (6(\lambda_0 + \mu_0 + \sigma_0)U_\theta - 4(\mu_0 + \lambda_0 + 2\sigma_0)U_r) - 6\gamma \frac{R^3}{r^4} (2U_r - U_\theta) \right] \sin^2 \theta \cos 2\varphi \end{aligned}$$

where $\gamma = (3\chi_0 + 5\zeta_0)/R^3$.

The first and third equations of Eqs. (5.10) are identical to the corresponding equations involved in Eqs. (B3) from Zemlyanova and Mogilevskaya (2018a). The second equation of Eqs. (5.10) is corrected version of the second equation involved in Eqs. (B3) from the same paper, which had a misprint that, however, have not affected the results presented there.

The use of Eqs. (5.10) together with the conditions of continuity of displacements across the boundary of the sphere leads to the linear system of four equations to find the unknown coefficients Eqs.(2.4)-(2.5). This linear system and its solution are presented in the Appendix C.

To illustrate the effects of the Steigmann-Ogden interface parameters, we consider the example similar to that presented in Zemlyanova and Mogilevskaya (2018a) that involves a cavity of radius $R = 5 \text{ nm}$ and assume that the normalized simple shear stress at infinity is

$$\sigma_d/\mu = 0.000028818 \quad (5.11)$$

We also adopt the following three values of the normalized surface tension:

$$\sigma_0/\mu R = 0, \quad \sigma_0/\mu R = 0.0067435, \quad \sigma_0/\mu R = 0.0097983 \quad (5.12)$$

The rest of the parameters for the example are chosen to be identical to the following ones used in Zemlyanova and Mogilevskaya (2018a):

$$\nu = 0.3, \mu_0/\mu R = 0.030156, \lambda_0/\mu R = 0.060312, \gamma/\mu = 0.00028382 \quad (5.13)$$

On Fig. 2, we plotted the normalized hoop stress $\sigma_{\theta\theta}/\mu$ along the meridian line $\varphi = 0$ at the cavity surface ($0 \leq \theta \leq \pi/2$). It can be seen that the surface tension has significant effect on the normalized hoop stress variation. The normalized stress becomes compressive when $\sigma_0 \neq 0$ and its absolute value increases with the increase in the surface tension. It could also be observed from the plots of Fig. 2 that, for this special case of simple shear far-field load, the variation of the hoop stress with the angle θ is small with the maximum (minimum) achieved at $\theta = 0$ ($\theta = \pi/2$), respectively.

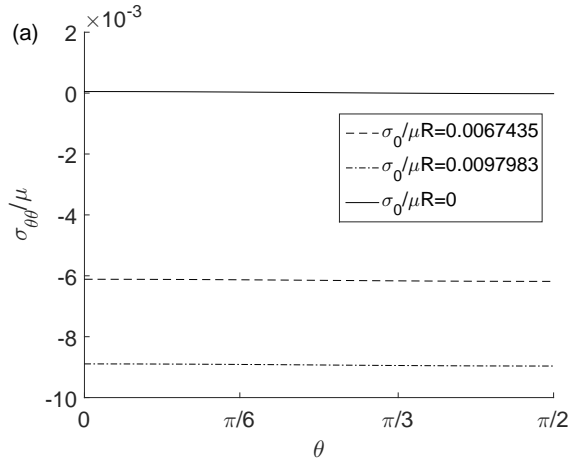


Fig. 2 Normalized hoop stress $\sigma_{\theta\theta}/\mu$ along the cavity surface, $\varphi = 0$

The normalized stress σ_{zz}/μ along the same meridian line $\varphi = 0$ at the cavity surface is plotted on Fig. 3. Here too, the surface tension has significant effect on the stress variation reaching its maximum at $\theta = 0$ and minimum at $\theta = \pi/2$. We also notice that, for the simple shear far-field load, the variation of σ_{zz}/μ with the angle θ is more pronounced than that of $\sigma_{\theta\theta}/\mu$.

To illustrate size-dependence of the surface related stresses, consider an additional example of the matrix made from anodic alumina ($\mu = 34.7\text{GPa}$ and $\nu = 0.3$) containing the cavity whose radius varies from $R = 5\text{nm}$ to $R = 20\text{nm}$. We fix the value of surface tension as $\sigma_0 = 1.7\text{N/m}$ and that of the simple shear stress as $\sigma_d = 100\text{MPa}$. The value of R -independent parameter parameter γ is chosen to be the same as the corresponding expression in Eq. (5.13), while the remaining parameters are chosen as

$$\mu_0 = 5.2321\text{N/m}, \lambda_0 = 10.4641\text{N/m} \quad (5.14)$$

which for $R = 5\text{nm}$ are consistent with the parameters used in expressions of Eq. (5.13).

Fig. 4 illustrates the variation of the normalized hoop stress $\sigma_{\theta\theta}/\sigma_d$ along the line $\varphi = \pi/2$ at the cavity surface ($0 \leq \theta \leq \pi/2$) for various values of R . For comparison, we also plotted

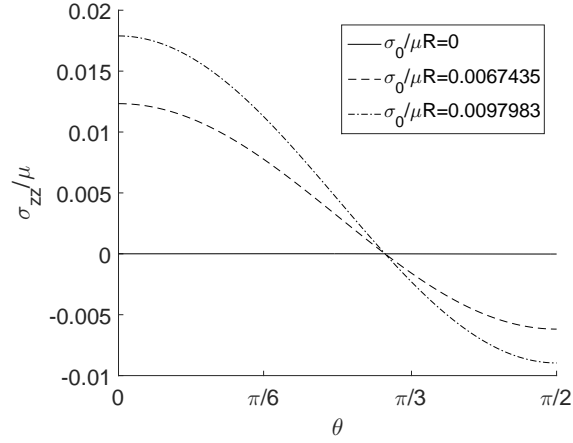


Fig. 3 Normalized stress σ_{zz}/μ along the cavity surface, $\varphi = 0$

the variation of the same but size-independent stress for the classical case (without surface effects). It can be seen from the plots on Fig.4 that the influence of surface effects on the normalized hoop stress diminishes with the increase in R .

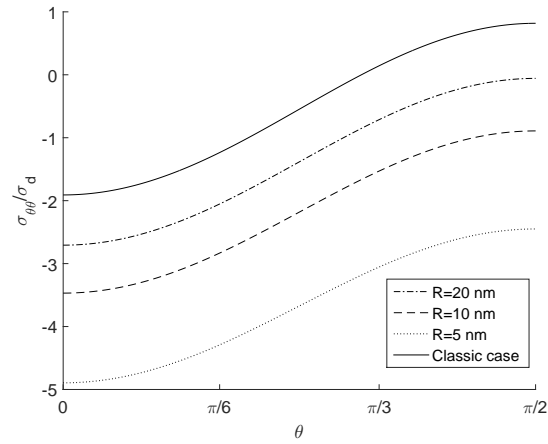


Fig. 4 Normalized hoop stress $\sigma_{\theta\theta}/\sigma_d$ along the cavity surface, $\varphi = \pi/2$

6. Effective properties of the isotropic particulate composites with the complete Steigmann-Ogden model of interfaces

The new analytical solution of previous section will now be used to derive the single-inhomogeneity-based approximation formula for the effective shear modulus of

macroscopically isotropic composites containing spherical inhomogeneities with the interfaces described by the complete Steigmann-Ogden model. Similar formula for the effective bulk modulus was reported in Zemlyanova and Mogilevskaya (2018a,b).

To obtain shear modulus μ_{ef} , we will use Maxwell's (1873) concept of equivalent inhomogeneity, see e.g. McCartney (2010), Mogilevskaya et al. (2012), and apply the same two-stage procedure as in Mogilevskaya et al. (2018) and Zemlyanova and Mogilevskaya (2018a,b).

On the first stage, the problem involving a composite system containing an inhomogeneity with the complete Steigmann-Ogden interface and subjected to simple shear far-field load is solved twice, once with both the external load and surface tension included and the second time with just surface tension. The solution of the second problem is then subtracted from that for the first problem. This procedure is needed to eliminate the residual effects due to the presence of the surface tension, see Mogilevskaya et al. (2010). As the results, the displacements in the matrix will be given by Eqs. (4.15)-(4.18) with $D_0 = 0$ and remaining coefficients found from the system of Eqs. (C1)-(C2) of Appendix C.

Then, we equate the coefficient D_4 for the leading $1/r^2$ (dipole) term in the obtained displacements with that related to the problem involving the equivalent perfectly bonded inhomogeneity of the same radius with the unknown shear modulus μ_{eq} to find the value of that modulus.

On the second stage, the obtained modulus of the equivalent inhomogeneity could be used in any single-inhomogeneity-based homogenization scheme for perfectly bonded spherical particles. Here, we will use the following Maxwell type approximation formulae, McCartney (2010):

$$\frac{\mu_{ef}}{\mu} = \frac{\mu_{eq} + \mu^* + c\mu^*(\mu_{eq}/\mu - 1)}{\mu_{eq} + \mu^* - c(\mu_{eq} - \mu)} \quad (6.1)$$

with c being the volume fraction of the equivalent inhomogeneity and

$$\mu^* = \mu \frac{9K + 8\mu}{6(K + 2\mu)} = \frac{\mu}{2} \frac{9\lambda + 14\mu}{3\lambda + 8\mu} \quad (6.2)$$

The solution for the problem of perfectly bonded inhomogeneity can be extracted from Eq. (4.18) by assuming vanishing surface parameters. The coefficient for the leading $1/r^2$ (dipole) term for that case is $(5 - 4\nu) D_4^{eq} / (1 - 2\nu)$ in which

$$D_4^{eq} = -\frac{5}{2} \frac{(\mu_{eq}/\mu - 1) \sigma_d^\infty R^3}{(9\lambda + 14\mu) + 2(\mu_{eq}/\mu)(8\lambda + 3\mu)} \quad (6.3)$$

with $\lambda = K^{(3)} - 2\mu/3$.

Thus, assuming that $D_4^{eq} = D_4^{S-O}$, μ_{eq} could be obtained as

$$\frac{\mu_{eq}}{\mu} = 1 - 2R^{-3} \frac{4\mu + 5\lambda}{1 + 4(D_4 R^{-3} / \sigma_d^\infty)(3\mu + 8\lambda) / 5} \frac{D_4^{S-O}}{\sigma_d^\infty} \quad (6.4)$$

in which $D_4^{S-O} / \sigma_d^\infty$ can be found from Eqs. (C4) of Appendix C.

Using the following notation:

$$\Lambda = \frac{2 + 5\lambda/2\mu}{\mu + 4\mu (D_4^{S-O} R^{-3}/\sigma_d^\infty) (3\mu + 8\lambda)/5} \frac{D_4^{S-O} R^{-3}}{\sigma_d^\infty} \quad (6.5)$$

and substituting Eq. (6.4) into Eq. (6.1), we obtain the following expression for the effective shear modulus μ_{ef} :

$$\frac{\mu_{ef}}{\mu} = 1 - \frac{15c(\lambda + 2\mu)\Lambda}{2(3\lambda + 8\mu)[1 - (1 - c)\Lambda] + (9\lambda + 14\mu)} \quad (6.6)$$

To illustrate the effects of the Steigmann-Ogden interface parameters on the effective shear modulus of the composite material with overall isotropy, we consider the example of the preceding section with the parameters given by Eqs. (5.11)-(5.13) and use Eq. (6.6) to estimate μ_{ef} . Fig. 4 presents the plots of the normalized effective shear modulus as a function of the volume fraction of the cavities; the plot for the classical case with $\mu_0 = \lambda_0 = \gamma = \sigma_0 = 0$ (solid line) is presented there as well. It could be seen from Fig. 4 that while the effects of surface elastic parameters lead to the increase in overall stiffness of the composite, the influence of surface tension is insignificant as its variation does not noticeable affect the value of μ_{ef}/μ .

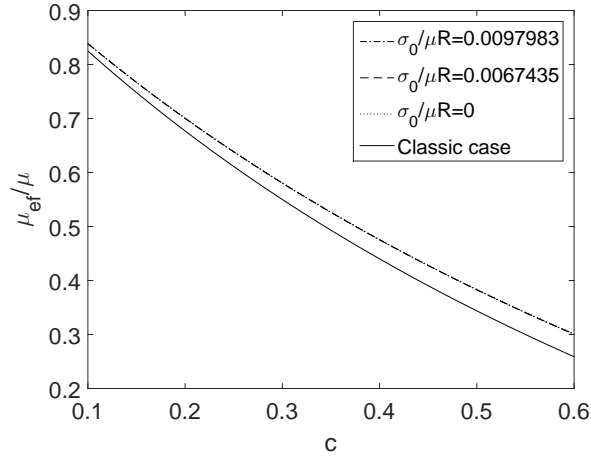


Fig. 5 Normalized effective shear modulus for the composite material with overall isotropy

To separate the influences of the *elastic* interface parameters, we assumed that $\sigma_0 = 0$ and evaluated, using the single-inhomogeneity based estimate of Eq. (6.6), the values of the normalized effective shear modulus for three different cases: i) classical case with no surface effects, ii) the case with $\gamma/\mu = 0$ (G-M model), and iii) the case with $\gamma/\mu = 0.00028382$ (S-O model). The remaining elastic parameters were taken from the corresponding expressions of Eq. (5.13). The estimates for all three cases are presented in the Table 1 for three values of the volume fractions.

It could be seen from the table that, for the parameters considered, the combined influence

Table 1 Normalized shear modulus for the three interface models

c	μ_{ef}/μ		
	Classic case	G-M model	S-O model
0.1	0.825	0.838878	0.838930
0.3	0.550	0.580938	0.581057
0.5	0.34375	0.383570	0.383725

of the surface elasticity parameters μ_0 , λ_0 on the normalized effective shear modulus is significantly larger than the influence of the bending parameter γ , especially for the smaller volume fractions of the cavities.

7. Conclusions

This paper presents two new important contributions to the studies of the surface/interface effects in heterogeneous media.

The first contribution is the analytical representations similar to those of Christensen and Lo (1979) that could be used for solutions of various problems involving spherical and circular material surfaces that possess constant surface tension. These representations are derived here for the first time. While in the present paper we used them for the analysis of two specific interface models, we envision that they could be used for the analysis of various Eshelby-type problems, including new problems that might emerge in studies of surface effects. The obtained representations significantly simplify the solutions of such problems and can be useful in the comparative studies of various surface/interface models and their influences on the local behavior of the fiber- and particle reinforced nano composites. They should be especially valuable for the researchers of engineering community as they are presented in ready-to use forms and require relatively little algebra. In addition, they could be extremely valuable to the researchers in the area of Micromechanics as they allow for easy construction of various single-inhomogeneity-based estimates for overall properties of such materials.

The second contribution is the new analytical solution of the problem of a spherical inhomogeneity with the interface described by the *complete* Steigmann-Ogden model. This solution is important for the analysis of the local and overall behavior of nano-scale materials and, at the very least, the investigators who want to numerically solve more complicated problems involving material surfaces could utilize our solution as benchmark example. This solution was readily obtained with the use of the new Christensen and Lo's type representations for the displacements, while the alternative and may be more straightforward approach to obtain it would require the use of tedious algebra of spherical harmonics. The attractive feature of this new solution is that all the coefficients involved in it are provided as closed-form analytical expressions. This allows for accurate identification of all governing dimensionless problem parameters and their influences on the solution.

Acknowledgements

The first author (S.M.) gratefully acknowledges the support provided by the Theodore W. Bennett Chair, University of Minnesota. The second author (V.K.) acknowledges the

support from Science and Technology Center in Ukraine (STCU), award #6247. The third author (A.Z.) gratefully acknowledges the support from Simons Collaboration grant, award # 319217.

APPENDIX A

The representations for the displacements for the problem of Fig.1a

The displacements in polar coordinates (Fig.1a) everywhere in the composite system can be expressed in terms of two Kolosov-Muskhelishvili potentials $\varphi(z)$ and $\psi(z)$ as, see Muskhelishvili (1959)

$$2\mu [u_r(z) + iu_\theta(z)] = \exp(-i\vartheta) \left[\kappa\varphi(z) - z\overline{\varphi'(z)} - \overline{\psi(z)} \right] \quad (\text{A1})$$

in which the elastic parameters μ and $\kappa = 3 - 4\nu$ are the parameters of the specific phase: (μ, κ) for the matrix or (μ_I, κ_I) for the inhomogeneity.

In Mogilevskaya et al. (2008) and Zemlyanova and Mogilevskaya (2018), it was shown that the potentials inside and outside of circular inhomogeneity are

inside the inhomogeneity ($z = r \exp(i\vartheta)$, $r < R$)

$$\begin{aligned} \varphi(z) &= \frac{2\mu_I}{\kappa_I - 1} ReA_1 \frac{r}{R} \exp(i\vartheta) + \frac{2\mu_I}{\kappa_I} A_3 \frac{r^3}{R^3} \exp(3i\vartheta) \\ \psi(z) &= -2\mu_I \left(\frac{3}{\kappa_I} A_3 + \overline{A_{-1}} \right) \frac{r}{R} \exp(i\vartheta) \end{aligned} \quad (\text{A2})$$

inside the matrix ($z = r \exp(i\varphi)$, $r > R$)

$$\varphi(z) = \frac{2}{\kappa + 1} \left(-\omega^{(1)} A_{-1} + 3\eta^{(2)} \overline{A_3} \right) \frac{R}{r} \exp(-i\vartheta) + \varphi^\infty(z) \quad (\text{A3})$$

$$\begin{aligned} \psi(z) &= \frac{2}{\kappa + 1} \left\{ (\kappa - 1) \left(\omega^{(0)} ReA_1 + \frac{\sigma_0}{2} \right) \frac{R}{r} \exp(-i\vartheta) \right. \\ &+ \left. \left[\left(\omega^{(1)} - \kappa\eta^{(2)} \right) A_{-1} + \omega^{(2)} \overline{A_3} \right] \frac{R^3}{r^3} \exp(-3i\vartheta) \right\} \\ &+ \psi^\infty(z) \end{aligned}$$

in which

$$ReA_1 = -\frac{1}{4\Delta_1} \sigma_0 + \frac{\kappa + 1}{4} \frac{1}{4\Delta_1} R (\sigma_{11}^\infty + \sigma_{22}^\infty) \quad (\text{A4})$$

$$A_{-1} = -\frac{\kappa + 1}{4} \frac{\mu\kappa_I + \mu_I + 3\kappa_I\eta^{(1)}}{\Delta_2} R (\sigma_{22}^\infty - \sigma_{11}^\infty - 2i\sigma_{12}^\infty)$$

$$A_3 = -\frac{\kappa + 1}{4} \frac{\kappa_I\eta^{(2)}}{\Delta_2} R (\sigma_{22}^\infty - \sigma_{11}^\infty + 2i\sigma_{12}^\infty)$$

$$\varphi^\infty(z) = \frac{\sigma_{11}^\infty + \sigma_{22}^\infty}{4} z, \quad \psi^\infty(z) = \frac{\sigma_{22}^\infty - \sigma_{11}^\infty + 2i\sigma_{12}^\infty}{2} z \quad (\text{A5})$$

and

$$\begin{aligned}
\Delta_1 &= \frac{\mu_I}{\kappa_I - 1} + \frac{\mu}{2} + \eta \\
\Delta_2 &= (\mu + \kappa\mu_I)(\mu\kappa_I + \mu_I) + \eta^{(1)} [3\kappa_I(\mu + \kappa\mu_I) + \kappa(\mu\kappa_I + \mu_I)] \\
&\quad + 12\kappa\kappa_I\eta \left(\frac{\sigma_0}{4R} + \gamma \right)
\end{aligned} \tag{A6}$$

Substituting the expressions of Eqs. (A2), (A3) into the representation of Eq. (A1) (with the corresponding elastic parameters) and performing some algebra, we obtain the representations for the displacements in the polar coordinate system as
inside the inhomogeneity

$$\begin{aligned}
u_r(z) + iu_\vartheta(z) &= ReA_1 \frac{r}{R} + A_3 \frac{r^3}{R^3} \exp(2i\vartheta) \\
&\quad + \left[\frac{3}{\kappa_I} \bar{A}_3 \left(\frac{r}{R} - \frac{r^3}{R^3} \right) + A_{-1} \frac{r}{R} \right] \exp(-2i\vartheta)
\end{aligned} \tag{A7}$$

inside the matrix

$$\begin{aligned}
u_r(z) + iu_\vartheta(z) &= \frac{1}{\mu(\kappa + 1)} \left\{ -(\kappa - 1) \left(\omega^{(0)} ReA_1 + \frac{\sigma_0}{2} \right) \frac{R}{r} \right. \\
&\quad + \kappa \left(-\omega^{(1)} A_{-1} + 3\eta^{(2)} \bar{A}_3 \right) \frac{R}{r} \exp(-2i\vartheta) \\
&\quad + \left(-\omega^{(1)} \bar{A}_{-1} + 3\eta^{(2)} A_3 \right) \frac{R}{r} \exp(2i\vartheta) \\
&\quad + \left[\left(-\omega^{(1)} + \kappa\eta^{(2)} \right) \bar{A}_{-1} - \omega^{(2)} A_3 \right] \frac{R^3}{r^3} \exp(2i\vartheta) \left. \right\} \\
&\quad + u_r^\infty(z) + iu_\vartheta^\infty(z)
\end{aligned} \tag{A8}$$

where $\exp(i\vartheta) = \cos \vartheta + i \sin \vartheta$

$$u_r^\infty(z) + iu_\vartheta^\infty(z) = (\kappa - 1) \frac{\sigma_{11}^\infty + \sigma_{22}^\infty}{8\mu} r - \frac{\sigma_{22}^\infty - \sigma_{11}^\infty - 2i\sigma_{12}^\infty}{4\mu} r \exp(-2i\vartheta) \tag{A9}$$

$$\omega^{(0)} = \frac{2\mu_I}{\kappa_I - 1} - \frac{2\mu}{\kappa - 1} + 2\eta = K_I^{(2)} - K^{(2)} + 2\eta \tag{A10}$$

$$\omega^{(1)} = \mu_I - \mu + \eta^{(1)} \tag{A11}$$

$$\omega^{(2)} = \mu_I \frac{\kappa}{\kappa_I} - \mu + 3\kappa\eta^{(1)} + 3\eta^{(2)} \tag{A12}$$

$$\eta^{(1)} = \eta + \gamma + \sigma_0/4R \tag{A13}$$

$$\eta^{(2)} = \eta - \gamma - \sigma_0/4R \tag{A14}$$

$$\eta = \frac{2\mu_0 + \lambda_0}{4R} \tag{A15}$$

and the remaining parameters are defined by Eqs. (A4)-(A6) .

From Eq. (A4), it follows that, for the case of simple shear far-field load ($\sigma_{11}^\infty = -\sigma_{22}^\infty = \sigma_d^\infty$, $\sigma_{12}^\infty = 0$), the coefficients involved in Eqs. (A7), (A8) are

$$\begin{aligned} ReA_1 &= -\frac{\sigma_0}{2\left(K_I^{(2)} + \mu + 2\eta\right)} \\ A_{-1} &= \frac{\kappa + 1}{2} \frac{\mu\kappa_I + \mu_I + 3\kappa_I\eta^{(1)}}{\Delta_2} R\sigma_d^\infty \\ A_3 &= \frac{\kappa + 1}{2} \frac{\kappa_I\eta^{(2)}}{\Delta_2} R\sigma_d^\infty \end{aligned} \quad (\text{A16})$$

where Δ_2 is defined in Eq. (A6).

APPENDIX B

Vector representations for the displacements for the problem of Fig.1b

The following vector partial solutions are involved in representations (4.10), (4.11):

$$\mathbf{u}_{00}^{(3)}(\mathbf{x}) = -2(1 - 2\nu)r\mathbf{S}_{00}^{(3)}/3, \quad \mathbf{u}_{22}^{(1)}(\mathbf{x}) = \frac{r}{24}\left(\mathbf{S}_{22}^{(1)} + 2\mathbf{S}_{22}^{(3)}\right), \quad \mathbf{u}_{22}^{(3)}(\mathbf{x}) = \frac{r^3}{24}\left[\frac{7-4\nu}{21}\mathbf{S}_{22}^{(1)} + \frac{4\nu}{7}\mathbf{S}_{22}^{(3)}\right] \quad (\text{B1})$$

$$\mathbf{U}_{00}^{(1)}(\mathbf{x}) = -\frac{1}{r^2}\mathbf{S}_{00}^{(3)}, \quad \mathbf{U}_{22}^{(1)}(\mathbf{x}) = \frac{1}{r^4}\left(\mathbf{S}_{22}^{(1)} - 3\mathbf{S}_{22}^{(3)}\right), \quad \mathbf{U}_{22}^{(3)}(\mathbf{x}) = \frac{1}{3r^2}\left[(1 - 2\nu)\mathbf{S}_{22}^{(1)} + (5 - 4\nu)\mathbf{S}_{22}^{(3)}\right] \quad (\text{B2})$$

in which the vector spherical surface harmonics $\mathbf{S}_{ts}^{(i)}$ (Morse and Feshbach, 1953)

$$\mathbf{S}_{ts}^{(1)} = \mathbf{e}_\theta \frac{\partial}{\partial \theta} \chi_t^s + \frac{\mathbf{e}_\varphi}{\sin \theta} \frac{\partial}{\partial \varphi} \chi_t^s, \quad \mathbf{S}_{ts}^{(2)} = \frac{\mathbf{e}_\theta}{\sin \theta} \frac{\partial}{\partial \varphi} \chi_t^s - \mathbf{e}_\varphi \frac{\partial}{\partial \theta} \chi_t^s, \quad \mathbf{S}_{ts}^{(3)} = \mathbf{e}_r \chi_t^s. \quad (\text{B3})$$

are expressed via the scalar surface harmonics $\chi_t^s(\theta, \varphi)$ as

$$\chi_t^s(\theta, \varphi) = P_t^s(\cos \theta) \exp(is\varphi) \quad (\text{B4})$$

and $P_t^s(\cos \theta)$ are associated Legendre polynomials.

The constants $D_0, D_3, D_4, A_0, A_1, A_2$ of Eqs. (4.12)-(4.17) are found from the system of linear equations that represent the interface and far-field conditions (Kushch et al., 2011, Kushch, 2013). In our notations, they are

- continuity of displacements

$$\begin{aligned} \frac{1}{R^3}D_0 &= A_0 \\ \frac{\sigma_d^\infty}{4\mu} - \frac{2}{R^5}D_3 + \frac{2}{R^3}D_4 &= A_1 - R^2 \frac{7-4\nu_I}{1-2\nu_I} A_2 \\ \frac{\sigma_d^\infty}{4\mu} + \frac{3}{R^5}D_3 + \frac{1}{R^3} \frac{5-4\nu}{1-2\nu} D_4 &= A_1 - R^2 \frac{6\nu_I}{1-2\nu_I} A_2 \end{aligned} \quad (\text{B5})$$

- interface conditions of Eqs. (4.1)-(4.3)

$$\begin{aligned} \frac{2}{R^3}D_0 &= -\frac{\mu_I}{\mu} \frac{(1+\nu_I)}{(1-2\nu_I)}A_0 - f_0 & (B6) \\ \frac{\sigma_d^\infty}{4\mu} + \frac{2}{R^3} \left(\frac{4}{R^2}D_3 + \frac{1+\nu}{1-2\nu}D_4 \right) &= \frac{\mu_I}{\mu} \left(A_1 - R^2 \frac{7+2\nu_I}{1-2\nu_I}A_2 \right) - 6f_1 \\ \frac{\sigma_d^\infty}{4\mu} + \frac{2}{R^3} \left(-\frac{6}{R^2}D_3 + \frac{\nu-5}{1-2\nu}D_4 \right) &= \frac{\mu_I}{\mu} \left(A_1 + R^2 \frac{3\nu_I}{1-2\nu_I}A_2 \right) - 3f_2 \end{aligned}$$

In Eq. (B6),

$$\begin{aligned} f_0 &= -\frac{\sigma_0}{\mu R} + \frac{\eta_0}{\mu R}A_0 & (B7) \\ f_1 &= \frac{(\mu_0 - \sigma_0) - 3(\lambda_0 + 2\mu_0)}{6\mu R} \left(A_1 - R^2 \frac{7-4\nu_I}{1-2\nu_I}A_2 \right) \\ &\quad + \frac{\lambda_0 + \mu_0 + \sigma_0}{3\mu R} \left(A_1 - R^2 \frac{6\nu_I}{1-2\nu_I}A_2 \right) \\ f_2 &= \frac{\lambda_0 + \mu_0 + \sigma_0}{\mu R} \left(A_1 - R^2 \frac{7-4\nu_I}{1-2\nu_I}A_2 \right) \\ &\quad - 2\frac{\lambda_0 + \mu_0 + 2\sigma_0}{3\mu R} \left(A_1 - R^2 \frac{6\nu_I}{1-2\nu_I}A_2 \right) \end{aligned}$$

in which η_0 is defined by Eq. (4.19).

After some algebraic manipulations with Eqs. (B5)-(B7), one can arrive to the following expressions for the coefficients A_0 , D_0 :

$$A_0 = D_0/R^3 = \frac{2\sigma_0/R}{4\mu + 3K_I^{(3)} + 2\eta_0} \quad (B8)$$

The analytical expressions for the remaining coefficients will be presented in Appendix C as a particular case of more general expressions for the coefficients related to the Steigmann-Ogden model.

APPENDIX C

Coefficients involved in the representations of Eqs. (2.4), (2.5)

The continuity conditions for the displacements produce two linear equations for the unknown coefficients A_1 , A_2 , D_3 , D_4 in the representations of Eqs. (2.4), (2.5), (4.12)-(4.17):

$$A_1R - 3\frac{\lambda_I}{\mu_I}A_2R^3 - 3D_3R^{-4} - \frac{3\lambda + 5\mu}{\mu}D_4R^{-2} = D_1R \quad (C1)$$

$$A_1R - \frac{5\lambda_I + 7\mu_I}{\mu_I}A_2R^3 + 2D_3R^{-4} - 2D_4R^{-2} = D_1R$$

Substitution of the representations of Eqs. (2.4), (2.5), (4.12)-(4.17) into Eqs. (5.1)-(5.3) results in the following two additional linear equations for the unknown constants A_1 , A_2 , D_3 , D_4 :

$$C_{31}A_1R + C_{32}A_2R^3 - 24\mu D_3R^{-4} - (18\lambda + 20\mu)D_4R^{-2} = -2\mu D_1R \quad (C2)$$

$$C_{41}A_1R + C_{42}A_2R^3 + 8\mu D_3R^{-4} + (3\lambda + 2\mu)D_4R^{-2} = -\mu D_1R$$

where the parameters C_{31} , C_{32} , C_{41} , C_{42} are

$$\begin{aligned}
C_{31} &= -2\mu_I + \frac{2}{R}(\lambda_0 + \mu_0 - \sigma_0) - 6\gamma \\
C_{32} &= -3\lambda_1 - \frac{6}{R}(\lambda_0 + \mu_0) \frac{3\lambda_I + 7\mu_I}{\mu_I} - \frac{6}{R}\sigma_0 \frac{\lambda_I + 7\mu_I}{\mu_I} + 6\gamma \frac{\lambda_I - 7\mu_I}{\mu_I} \\
C_{41} &= -\mu_I - \frac{1}{R}(3\mu_0 + \lambda_0 - \sigma_0) + \gamma \\
C_{42} &= 8\lambda_I + 7\mu_I + \frac{\mu_0}{R} \frac{19\lambda_I + 35\mu_I}{\mu_I} + 3 \frac{\lambda_0}{R} \frac{3\lambda_I + 7\mu_I}{\mu_I} - \frac{\sigma_0}{R} \frac{\lambda_I - 7\mu_I}{\mu_I} - \gamma \frac{\lambda_I - 7\mu_I}{\mu_I}
\end{aligned} \tag{C3}$$

As the Steigmann-Ogden model reduces to that of Gurtin-Murdoch, Eqs. (C1)-(C3) should reproduce the corresponding equations of Eqs. (B5)-(B7), when the bending parameters vanish, i.e. $\gamma = 0$. After some algebraic manipulations, not shown here, we have verified that this was, indeed, the case.

The system of Eqs. (C1)-(C2) can be solved analytically leading to the following expressions for the coefficients A_1 , A_2 , D_3 , D_4 :

$$\begin{aligned}
A_1/D_1 &= F(E_{22} - E_{12})/(E_{11}E_{22} - E_{12}E_{21}) \\
A_2/D_1 &= F(E_{11} - E_{21})R^{-2}/(E_{11}E_{22} - E_{12}E_{21}) \\
D_3/D_1 &= - [(A_1/D_1) ((3\lambda + 2\mu)C_{31} + (18\lambda + 20\mu)C_{41}) R^5 \\
&\quad + (A_2/D_1) ((3\lambda + 2\mu)C_{32} + (18\lambda + 20\mu)C_{42}) R^8 + 24\mu(\mu + \lambda)R^5] (8\mu)^{-1} (9\lambda + 14\mu)^{-1} \\
D_4/D_1 &= [(A_1/D_1) (C_{31} + 3C_{41})R^3 + (A_2/D_1) (C_{32} + 3C_{42})R^5 + 5\mu R^3] (9\lambda + 14\mu)^{-1}
\end{aligned} \tag{C4}$$

where the parameters E_{11} , E_{12} , E_{21} , E_{22} , F are given by

$$\begin{aligned}
E_{11} &= 1 - [(3\lambda + 10\mu)C_{31} + (18\lambda + 44\mu)C_{41}] (4\mu)^{-1} (9\lambda + 14\mu)^{-1} \\
E_{12} &= - [(3\lambda + 10\mu)C_{32} + (18\lambda + 44\mu)C_{42}] (4\mu)^{-1} (9\lambda + 14\mu)^{-1} - (5\lambda_1 + 7\mu_1)/\mu_1 \\
E_{21} &= 1 - [(15\lambda + 34\mu)C_{31} + 6(3\lambda + 10\mu)C_{41}] (8\mu)^{-1} (9\lambda + 14\mu)^{-1} \\
E_{22} &= -3\lambda_1/\mu_1 - [(15\lambda + 34\mu)C_{32} + 6(3\lambda + 10\mu)C_{42}] (8\mu)^{-1} (9\lambda + 14\mu)^{-1} \\
F &= 15(\lambda + 2\mu)/(9\lambda + 14\mu)
\end{aligned} \tag{C5}$$

References

- [1] Y. Benveniste, G.J. Dvorak, T. Chen. Stress fields in composites with coated inclusions. *Mech. Mater.* 7, (1989), 305-317.
- [2] J.W. Cahn, F. Larch. Surface stress and the chemical equilibrium of small crystals—II. Solid particles embedded in a solid matrix. *Acta Metall.* 30, (1982), 51-56.
- [3] G. Chatzigeorgiou, F. Meraghni, A. Javili. Generalized interfacial energy and size effects in composites. *J. Mech. Phys. Solids* 106, (2017), 257-282.
- [4] P. Chhapadia, P. Mohammadi, P. Sharma. Curvature-dependent surface energy and implications for nanostructures. *J. Mech. Phys. Solids* 59, (2011), 2103-2115.
- [5] R.M. Christensen, K.H. Lo. Solutions for effective shear properties in three phase sphere and cylinder models. *J. Mech. Phys. Solids* 27, (1979), 315-330.
- [6] R. Dingreville, J.M. Qu, M. Cherkaoui. Surface free energy and its effect on the elastic behavior of nano-sized particles. *J. Mech. Phys. Solids* 53, (2005), 1827-1854.

- [7] H.L. Duan, J. Wang, Z.P. Huang, B.L. Karihaloo. Size-dependent effective elastic constants of solids containing nano-inhomogeneities with interface stress. *J. Mech. Phys. Solids* 53, (2005), 1574-1596.
- [8] H.L. Duan, J. Wang, B.L. Karihaloo, Z.P. Huang. Nanoporous materials can be made stiffer than non-porous counterparts by surface modification. *Acta Materialia* 54, (2006), 2983-2990.
- [9] H.L. Duan, X. Yi, Z.P. Huang, J. Wang. A united scheme for prediction of effective moduli of multiphase composites with interface effects. Part I: Theoretical framework. *Mech. Mater.* 39, (2007), 81-93.
- [10] J.N. Goodier. Concentration of stress around spherical and cylindrical inclusions and flaws. *J. Appl. Mech.* 55, (1933), 39-44.
- [11] M.E. Gurtin, A.I. Murdoch. A continuum theory of elastic material surfaces. *Arch. Ration. Mech. Anal.* 57, (1975), 291-323.
- [12] M.E. Gurtin, A.I. Murdoch. Surface stress in solids. *Int. J. Solid. Struct.* 14, (1978), 431-440.
- [13] Z. Han, S.G. Mogilevskaya, D. Schillinger. Local fields and overall transverse properties of unidirectional composite materials with multiple nanofibers and Steigmann-Ogden interfaces. *Int. J. Solid. Struct.* 147, (2018), 166-182.
- [14] Z. Hashin. The spherical inclusion with imperfect interface. *J. Appl. Mech.* 58, (1991), 444-449.
- [15] L.H. He, Z.R. Li. Impact of surface stress on stress concentration. *Int. J. Solid. Struct.* 43, (2006), 6208-6219.
- [16] E. Herve, A. Zaoui. n-Layered inclusion-based micromechanical modelling. *Int. J. Engng. Sci.* 31, (1993), 1-10.
- [17] Huang, Z.P., Wang, J., 2006. A theory of hyperelasticity of multi-phase media with surface/interface energy effect. *Acta Mech.* 182, (1993), 195-210.
- [18] M. Jammes, S.G. Mogilevskaya, S.L. Crouch. Multiple circular nano-inhomogeneities and/or nano-pores in one of two joined isotropic elastic half-planes. *Eng. Anal. Bound. Elem.* 33, (2009), 233-248.
- [19] A. Javili, N.S. Ottosen, M. Ristinmaa, J. Mosler. Aspects of interface elasticity theory. *Math. Mech. Solids* 23, (2017), 1004-1024.
- [20] V.I. Kushch. *Micromechanics of composites: Multipole expansion approach.* Elsevier, (2013).
- [21] V.I. Kushch. Stress field and effective elastic moduli of periodic spheroidal particle composite with Gurtin-Murdoch interface. *Int. J. Eng. Sci.* 132, (2018), 79-96.
- [22] V.I. Kushch, V.S. Chernobai, G.S. Mishuris. Longitudinal shear of a composite with elliptic nanofibers: local stresses and effective stiffness. *Int. J. Eng. Sci.* 84, (2014), 79-94.
- [23] V.I. Kushch, S.G. Mogilevskaya, H.K. Stolarski, S.L. Crouch. Elastic interaction of spherical nanoinhomogeneities with Gurtin–Murdoch type interfaces. *J. Mech. Phys. Solids* 59, (2011), 1702=1716.
- [24] V.I. Kushch, S.G. Mogilevskaya, H.K. Stolarski. Elastic fields and effective moduli of particulate nanocomposites with the Gurtin-Murdoch model of interfaces. *Int. J. Solid. Struct.* 50, (2013), 1141-1153.
- [25] V.I. Kushch, S.V. Shmegeera, V.V. Mykhas'kiv. Multiple spheroidal cavities with surface stress as a model of nanoporous solid. *Int. J. Solid. Struct.* 152–153, (2018), 261-271.
- [26] C.W. Lim, Z.R. Li, L.H. He. Size dependent, non-uniform elastic field inside a nano-scale spherical inclusion due to interface stress. *Int. J. Solid. Struct.* 43, (2006), 5055-5065.

- [27] A.E.H. Love. *A Treatise on the Mathematical Theory of of Elasticity* (4th edn). University Press, Cambridge, (1927).
- [28] A.I. Lurie. *Theory of Elasticity*. Springer, New York (English translation of Russian 1970 edition, Nauka, Moscow), (2005).
- [29] J. C. Maxwell. *Treatise on Electricity and Magnetism*, vol. 1, Clarendon Press, Oxford (3rd edn), (1892).
- [30] L.N. McCartney. Maxwell's far-field methodology predicting elastic properties of multi-phase composites reinforced with aligned transversely isotropic spheroids. *Philos. Mag.* 90, (2010), 4175-4207.
- [31] C. Mi, D.A. Kouris. Nanoparticles under the influence of surface/interface elasticity. *Mech. Mater. Struct.* 1, (2006), 763-791.
- [32] R.E. Miller, V.B. Shenoy. Size-dependent elastic properties of nanosized structural elements. *Nanotechnology* 11, (2000), 139-147.
- [33] S.G. Mogilevskaya, S.L. Crouch, A. LaGrotta, H.K. Stolarski. The effects of surface elasticity and surface tension on the transverse overall elastic behavior of unidirectional nanocomposites. *Compos. Sci.* 70, (2010), 427-434.
- [34] S.G. Mogilevskaya, S.L. Crouch, H.K. Stolarski. Multiple interacting circular nanoinhomogeneities with surface/interface effects. *J. Mech. Phys. Solids* 56, (2008), 2298-2327.
- [35] S.G. Mogilevskaya, H.K. Stolarski, S.L. Crouch. On Maxwell's concept of equivalent inhomogeneity: when do the interactions matter? *J. Mech. Phys. Solids* 60, (2012), 391-417.
- [36] S.G. Mogilevskaya, A.Y. Zemlyanova, M. Zammarchi. On the elastic far-field response of a two-dimensional coated circular inhomogeneity: Analysis and applications. *Int. J. Solid. Struct.* 130-131, (2018), 199-210.
- [37] P.M. Morse, H. Feshbach. In: *Methods of Theoretical Physics*. McGraw-Hill, NewYork, (1953).
- [38] N.I. Muskhelishvili. *Some Basic Problems of the Mathematical Theory of Elasticity*. Noordhoff, Groningen, 1959.
- [39] C.Q. Ru. Simple geometrical explanation of Gurtin-Murdoch model of surface elasticity with clarification of its related versions. *Sci. China Phys., Mech. & Astron.* 53, (2010), 536-544.
- [40] G.N. Savin. *Stress concentrations around holes*. Pergamon Press, Oxford, (1961).
- [41] P. Sharma, S. Ganti. Interfacial elasticity corrections to size-dependent strain-state of embedded quantum dots. *Phys. Status Solidi* 234, (2002), R10-R12.
- [42] P. Sharma, S. Ganti. Size-dependent Eshelby's tensor for embedded nano-inclusions incorporating surface/interface energies. *J. Appl. Mech.* 71, (2004), 663-671.
- [43] P. Sharma, S. Ganti, N. Bhate. Effect of surfaces on the size-dependent elastic state of nano-inhomogeneities. *Appl. Phys. Lett.* 82, (2003), 535-537.
- [44] D.J. Steigmann, R.W. Ogden. Plain deformations of elastic solids with intrinsic boundary elasticity. *Proc. R. Soc. London A* 453, (1997), 853-877.
- [45] D.J. Steigmann, R.W. Ogden. Elastic surface-substrate interactions. *Proc. R. Soc. London A* 455, (1999), 437-474.
- [46] Y. Xu, Q-C. He, S-T. Gu. Effective elastic moduli of fiber-reinforced composites with interfacial displacement and stress jumps. *Int. J. Solids Struct.* 80, (2016), 146-157.
- [47] A.Y. Zemlyanova, S.G. Mogilevskaya. On spherical inhomogeneity with Steigmann-Ogden interface. *J. Appl. Mech.* 85, (2018a), 121009-121009-10.

- [48] A.Y. Zemlyanova, S.G. Mogilevskaya. Circular inhomogeneity with Steigmann–Ogden interface: Local fields, neutrality, and Maxwell’s type approximation formula. *Int. J. Solids Struct.* 135, (2018b), 85-98.

List of Figures

- Fig. 1. a) Circular and b) spherical inhomogeneity in an infinite matrix
Fig. 2. Normalized hoop stress $\sigma_{\theta\theta}/\mu$ along the cavity surface, $\varphi = 0$
Fig. 3. Normalized stress σ_{zz}/μ along the cavity surface, $\varphi = 0$
Fig. 4. Normalized hoop stress $\sigma_{\theta\theta}/\sigma_d$ along the cavity surface, $\varphi = \pi/2$
Fig. 5. Normalized effective shear modulus for the composite material with overall isotropy

List of Tables

- Table 1. Normalized shear modulus for the three interface models